Preprints (www.preprints.org) | NOT PEER-REVIEWED | Posted: 4 April 2018 doi:10.20944/preprints201804.0055.v1

Article

Prediction vs. Performance of IDF curves from precipitation data of regional climate models for a Brazilian coastal county

Daniela Martins[1,*], Nadiane Smaha Kruk[1], Paulo Ivo Braga de Queiroz[2], Wilson Cabral de Souza Júnior[1] and Gabriele Vanessa Tschöke[3]

[1] Water Resources and Environmental Sanitation Department. Aeronautics Institute of Technology – São José dos Campos, SP - Brazil.
[2] Geotechnics Department. Aeronautics Institute of Technology – São José dos Campos, SP – Brazil.
[3] Federal University of Paraná – Curitiba, PR - Brazil
* Correspondence: engdanimartins@gmail.com; Tel.: +55-12-99165-5400

Abstract: Drainage systems are usually dimensioned for design storms based on intensity-duration-frequency (IDF) curves of extreme precipitation. For each location, different IDF curves are established based on local hydrological conditions. Recent research shows that these curves also vary with time, and should be updated with recent data. The purpose of this study is to evaluate IDF curves obtained from precipitation simulations from the Eta RCM, comparing them with IDF curves obtained from data of a rainfall station. Climate models can be a useful tool for assessing the impacts of climate changes on drainage systems, referring precipitation forecasts. In this study, the Eta RCM was forced by two global climate models: HadGEM2-ES and MIROC5. The bias of the precipitation data, generated by RCM models, was corrected using a Gamma distribution. The Juqueriquerê River Basin, in the cities of Caraguatatuba and São Sebastião, São Paulo State, Brazil, was chosen as a case study. The results show a good correlation between the IDF curves of simulated and observed rainfall for the control period (1960-2005), indicating the strong possibility of using the Eta RCM precipitation forecasts for 2007 - 2099 to establish future IDFs thereby, taking into account climate changes in urban drainage design.

Keywords: IDF curves, urban drainage, regional climate model, bias correction, climate changes.

---

1. Introduction

Estimates of extreme rainfall events magnitudes are essential components of hydrological risk analysis and design of urban infrastructures [41]. These estimates are usually performed via statistical techniques that have temporal stationarity as a fundamental hypothesis.

Several studies show that Earth's climate is changing and there is evidence that global temperature has been rising during the last century [15, 16, 34]. According to National Research Council [36], these changes in climate are the result of increased emissions of greenhouse gases like carbon dioxide (CO_2) from the burning of fossil fuels and destruction of tropical forests. As observed by Agilan and Umamehesh [1], nowadays it is widely recognized that global climate changes are intensifying extreme rainfall events and creating a non-stationary component in the extreme rainfall time series.

In addition to global warming and the increase of the frequency of El Niño events, there are other processes, which may also affect extreme rainfall incidence in urban areas, such as the urbanization process itself. Some surfaces absorb solar heat in excess, raising temperatures from 2 to 10 °C and forming the heat islands [1, 31]. These heat islands are challenging to model although some trials are aiming to do it [20, 33].

© 2018 by the author(s). Distributed under a Creative Commons CC BY license.

Preprints (www.preprints.org) | NOT PEER-REVIEWED | Posted: 4 April 2018 doi:10.20944/preprints201804.0055.v1

According to PBMC [16], the scientific uncertainties in projections of climate change are inherent to the climate system because they are the result of nonlinear interactions and complexities intrinsic to natural phenomena. One of these uncertainties is related to natural variability of the climate system; additionally, there are uncertainties in the climate models, which cannot include all parameters, such as the global and regional carbon balance. Finally, there are uncertainties related to the various scenarios proposed for the emission of greenhouse gases.

Global and regional climate modeling have shown significant advances in recent years in considering representation of processes and phenomena critical for the study of climate change. Brazil has excelled in this area, developing regional and global atmospheric and coupled ocean-atmosphere climate models [15] (These models results are available upon request [40]). According to Sordo-Ward et al. [47] the National Institute for Space Research (INPE, São Paulo, Brazil) started using and developing different versions of the Eta Model for regional climate simulations and projections and came to the conclusion that the Eta Model is capable of capturing the spatial and temporal patterns of precipitation and temperature compared to the observed data and precedent studies for the La Plata basin.

Several studies indicate that, due to climate change, the hydrologic variables must be reviewed. Researchers developed futures intensity-duration-frequency (IDF) curves using model simulation (global or regional) [27, 39, 43, 48, 52]. For example, Solaiman and Simonovic [46] presented a methodology for updating the rainfall IDF curves for the City of London incorporating various uncertainties associated with the assessment of climate change impacts on a local scale. The results indicate that rainfall patterns in the City of London will most certainly change in future due to climate change. However, large uncertainties on projected rainfall intensity from six climate models impose constraints to the support of strong conclusions about the expected changes on future in the state of Alabama, United States, as reported by Mirhosseini et al. [32]. In this context, one can also cite studies by Madsen et al. [25] for Denmark and by Kao and Ganguly [19].

Vasiljevic et al. [50], analyzing two different periods, (1970-1984) and (1985-2003), noticed that storm drainage pipes would need to be larger in diameter due to the increased design rainfall intensities. Liew et al. [24] reported the lack of long rainfall records, which is common in most Southeast Asia countries and leads to the improper designs of urban drainage systems. Their study was validated on a site in Java, Indonesia. The RCM simulations might offer not only climate tendencies but also fill the lack of precipitation records.

Regarding to precipitation data forecasts, climate models can be a useful tool for assessing the impacts of climate changes on drainage systems.

The advantage of using a regional climate model (RCM), instead of a global one, is the increased spatial resolution, which can use finer grids in the area of interest and can better detail the topography of the region. This is possible through the technique of dynamic downscaling from global climate models (GCM).

Dynamic downscaling by Regional Climate Models (RCM) ensures consistency between climatological variables; however, they are computationally expensive [41]. According to Liew et al. [24], who validated the IDF curves for a site in Java (Indonesia), the optimal mitigation measures can be taken only when project rainfall is derived from RCM with high resolution.

Taking into account climate models predictions, it is possible to compare the results of simulations of a past period with observed data from rain gauge stations. However, according to Kuo et al. [22], rain gauge data are point measurements, expected to have larger temporal variability than RCM simulations, which give spatially averaged values. Data collected by rain gauges typically measure conditions over a small area (e.g., about 400 cm^2 or slightly larger) while an RCM grid point, depending on the domain resolution, can simulate precipitation over an area of several to hundreds of km^2 [4].

Therefore, one cannot expect a perfect match between gauge data and model simulations, because they represent different scales. Moreover, precipitation data simulated by climate models is a simplified version of nature and driven by coarse resolution input data, and thus climate model bias remains a critical problem, often requiring corrections before the model results can be

Preprints (www.preprints.org) | NOT PEER-REVIEWED | Posted: 4 April 2018 doi:10.20944/preprints201804.0055.v1

comparable to rain gauge measurements [13]. In order to decrease the gap between the climate model scales and the local urban drainage scales taking into account the inaccuracies in describing precipitation extremes, downscaling methods and bias-correction methods are commonly used in practice [52].

This work aims to evaluate IDF curves obtained from precipitation data simulated by the Eta regional climate model. The validation was done by comparing these curves with IDF curves obtained from observed data of the rain gauge station E2-046, which was the only station in that region with rain gauge data. E2-046 data range over 31 years.

2. Materials and Methods

In order to evaluate IDF curves obtained from the Eta RCM, precipitation data from 20-km horizontal resolution simulations were used. A study area was selected to compare the IDF adjustment from the RCM data with the IDF adjusted from observed data, during the period 1961 to 2005 (control period or baseline climate). The daily precipitation data simulated by Eta RCM were corrected for bias reduction by an accumulated bimodal, in which dry days were represented by a singled-value (zero) distribution, while rainy days were represented by a gamma distribution. This method was found to be more efficient in bias correction than power transformation [49].

As a study period of 31 years may be considered as a large one, both annual exceedances and annual maxima methods may be used in determining return period of extreme rainfalls [8]. In this work, the method of annual maxima was chosen.

It should be stressed that extremes distributions are usually different of probability distribution functions. In particular, all distributions that have exponential tail (which is the case of gamma distribution) have Gumbel frequency distribution (Type I) for the extreme values [13].

The practice of hydrological project usually faces the problem of data scarcity from recording type rain gauge. Daily total records from rainfall station are much easier to obtain, and they provide only accumulated daily rainfall records. This problem is even harder for climate forecasting via numerical models, which usually have internal time steps of three hours, and standard outputs of daily-accumulated rainfall data. In this paper, a simple disaggregation technique was adopted to estimate extreme rains for shorter periods [37].

As the IDF adjustment requires precipitation intensities for storm durations shorter than 24 hours, ratios given in the references were applied.

2.1. The Eta RCM Model

In order to obtain these forecasts for South America, regional climate model (RCM) simulations were performed with the Eta model [6, 7]. Eta model uses the Arakawa E Grid for horizontal discretization, which is a conservative finite difference (comparable to finite volume) scheme. Time integration uses a split-explicit technique [12] together with a forward-backward scheme due to [17]. Eta uses either the Betts-Miller-Janjíc [18] scheme for cumulus convection parameterization. Explicit precipitation is produced by a microphysics cloud scheme, which may be the Zhao [53] scheme. The longwave and shortwave parameterization schemes used were respectively the [11] and [23] schemes, as they were developed by the Geophysical Fluid Dynamics Laboratory (GFDL). The land-surface processes are represented by the NOAH scheme [10] with the annual cycle of vegetation greenness.

First, Eta model was nested in HadGEM2-ES (1.875°x1.250°, 38 levels) [9, 28], which is a global climate model developed by the Hadley Centre. Second, Eta was also nested in MIROC5 (1.4°x0.5-1.4°, 40 levels) [51], which is a global climate model from the Japanese National Institute for Environmental Studies. Chou et al [6, 7] present several comparisons that attest Eta model capabilities in reproduction of regional patterns of precipitation.

Preprints (www.preprints.org) | NOT PEER-REVIEWED | Posted: 4 April 2018 doi:10.20944/preprints201804.0055.v1

2.2. Study Region

The study region is the northern coast of São Paulo state, more specifically the Juqueriquerê River basin region (latitude 23°38'00"S and longitude 45°26'00"W), located in the municipalities of Caraguatatuba and São Sebastião, as shown in Figure 1. For the city of Caraguatatuba, a recent study determined two intensity-duration-frequency curves [29].

Aiming at obtaining a time series of precipitation within the study area, a rain gauge station with daily rainfall data named E2-046 was selected by the Information System for Management of Water Resources of the State of Sao Paulo (SigRH <http://www.sigrh.sp.gov.br>). The gauge, which has been providing daily rainfall data since 1943, is located within the Juqueriquerê River Basin (Figure 2) at an altitude of 20 m, latitude 23°38'00"S and longitude 45°26'00"W, and is still active. Values of maximum daily rainfall for each year from the rain gauge station are presented in Figure 3.

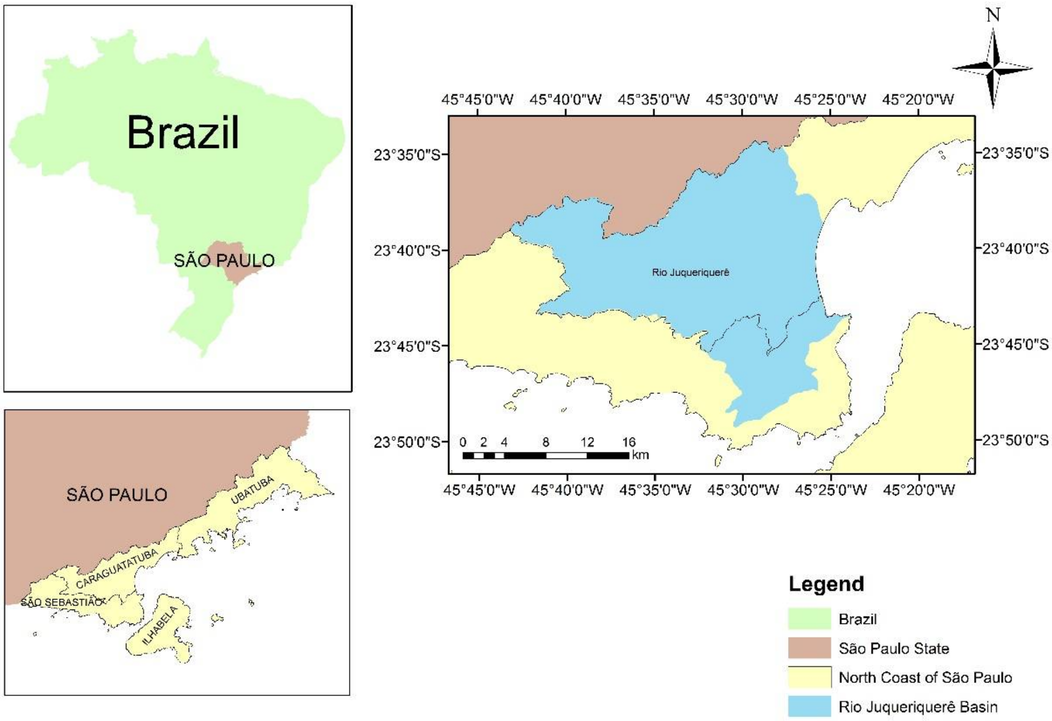

Figure 1: Location of the Juqueriquerê River Basin in Brazilian territory.

Preprints (www.preprints.org) | NOT PEER-REVIEWED | Posted: 4 April 2018 doi:10.20944/preprints201804.0055.v1

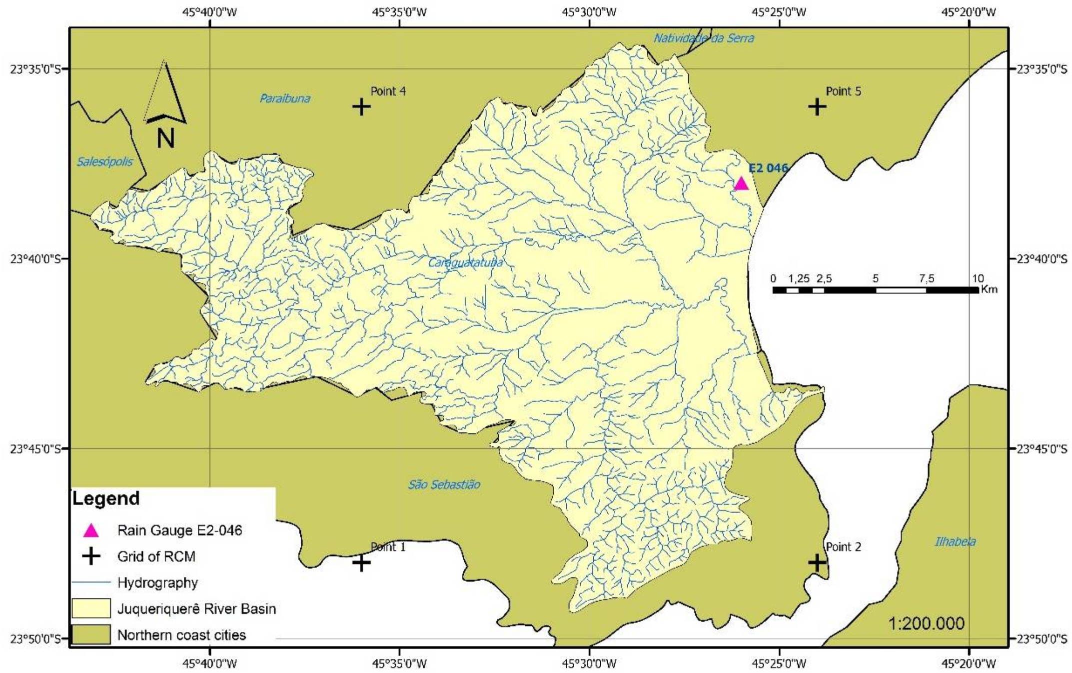

Figure 2: Map of the Juqueriquerê River Basin and grid points (dots) of the Eta RCM 20x20km model surrounding the E2-046 rainfall station.

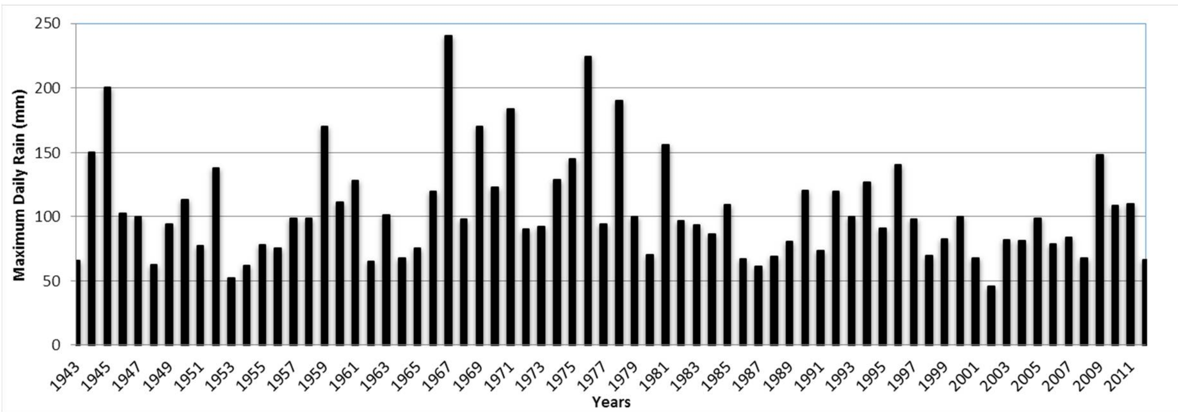

Figure 3: Maximum daily rainfall for each year for rain gauge station E2-046 (Caraguatatuba/SP) (70-year series)

RCM grid points were then selected (points 1 to 4, Figure 2). In order to compare the model simulations with the observations, the data from the four model grid points were interpolated to the E2-046 coordinates, using the inverse distance squared method. With the model and observed data now at the same point, the bias correction technique was applied to the simulated data.

2.3. Bias Correction

There are several methods to reduce bias. Tschöke et al. [49] used a bias correction technique based on the gamma distribution, which is assumed to be reliable for the distribution of precipitation events. Both the simulated and the observed distributions of rainfall intensities were considered to be very close to a gamma distribution. The distribution function is set excluding dry days, defined here as days with precipitation of less than 0.01 mm.

The gamma distribution, which is a frequency distribution with two parameters, is given by equation 1:

Preprints (www.preprints.org) | NOT PEER-REVIEWED | Posted: 4 April 2018 doi:10.20944/preprints201804.0055.v1

$$f(x) = \frac{x^{\gamma-1} e^{\frac{-x}{\beta}}}{\beta\gamma\Gamma(y)} \tag{1}$$

Where x is normalized daily precipitation, γ a shape parameter, β a scale parameter and Γ(y) is the complete gamma function.

The cumulative distribution function is set excluding dry days, that is, days with less precipitation than 0.01 mm. The transfer function is obtained by

$$X^{*}_{sim,val} = F_1^{-1}(F_2(X_{sim,val};\alpha_{sim,val};\beta_{sim,val});\alpha_{obs,cal};\beta_{obs,cal}), \tag{2}$$

where $X^{*}_{sim,val}$ is the corrected daily precipitation for the simulated data and validation period, α is a shape parameter and β a scale parameter. F is cumulative distribution function (F_1 is the cumulative gamma distribution function of observed values, while F_2 is the cumulative gamma distribution function of simulated values), X is the value of daily precipitation, X^* is the value of corrected daily precipitation and indexes *obs,val* and *sim,val* refer to observed values and simulated values of the validation period, respectively. [49].

This is the function that corrects the simulated precipitation events by equalizing the statistical distributions of precipitation values simulated for the validation period (1961 - 2005) with the statistical distributions of the observed values in the calibration period (1971 - 2001), as descripted in Figure 4 and equation 2.

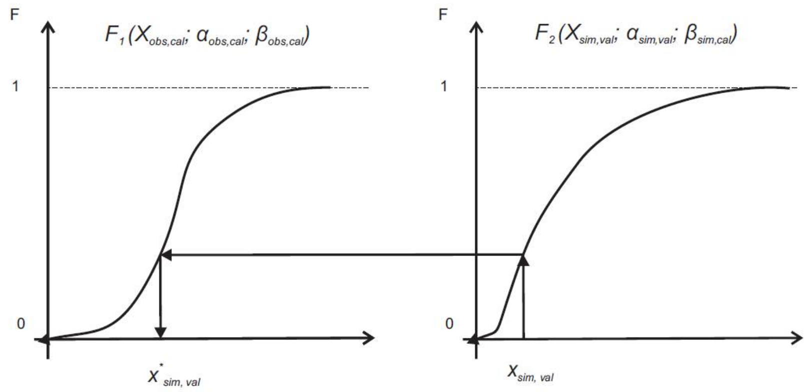

Figure 4: Maximum daily rainfall observed and simulated (with bias correction) at the E2-046 coordinates [49].

The annual maxima of the simulated daily precipitation data, referred to the E2-046 coordinates with bias correction, are presented in Figure 4. It is worth mentioning that the two nested climate models usually present different maximum values, which take place in different date. As an example, the maximum daily rainfall obtained from Eta-HadGEM2-ES model is 175 mm in 1996, while Eta-MIROC5 produced its higher value of 136 mm in 1986, as shown in Figure 5.

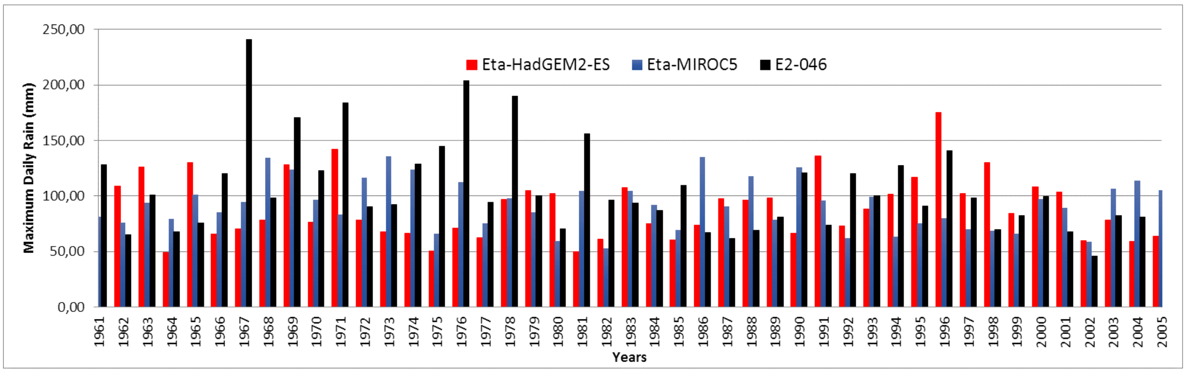

Figure 5: Maximum daily rainfall observed and simulated (with bias correction) at the E2-046 coordinates.

2.4. Frequency Analysis: The Gumbel Distribution

The objective of frequency analysis of hydrological variables is to relate the magnitude of the events to their frequency of occurrence through the use of a probability distribution. The results of frequency analysis are required to solve various engineering problems, such as, projects spillways of dams, bridges, culverts and flood control structures, and issues that involve estimating some characteristic value, such as minimum flow with 7-day and 10-year return period [24].

According to Magni [26], Gumbel was the first to employ extreme value theory in flood frequency analysis, yielding the so-called Gumbel distribution, also called an extreme value type 1 distribution, often used for predicting maximum events.

For extreme values of precipitation, it was used the Type 1 or Gumbel distribution. The cumulative probability function of the Gumbel distribution is given by [14] equation (3):

$$F_Y(y) = \exp\left[-\exp\left(-\frac{y-\beta}{\alpha}\right)\right] \tag{3}$$

For $-\infty<y<\infty$; $-\infty<\beta<\infty$ and $\alpha>0$.

Hence, a density distribution function of Gumbel is (4):

$$f_Y(y) = \frac{1}{\alpha}\exp\left[-\frac{y-\beta}{\alpha} - \exp\left(-\frac{y-\beta}{\alpha}\right)\right] \tag{4}$$

With the parameters expressed by:

$$\beta = \frac{\sqrt{6}}{\pi}\sqrt{VAR[Y]} \tag{5}$$

$$\alpha = E[Y] - 0.577\beta \tag{6}$$

Where α is the scale parameter and β the position parameter, E[Y] is the average and $VAR[Y]^{0,5}$ the standard deviation of the sample.

In the Gumbel distribution, as in [42] one has:

$$\frac{P(1_{day};T)-\alpha}{\beta} = -\ln\left(\ln\left(\frac{1}{F\left(P\left(day;T\right)\right)}\right)\right) \tag{7}$$

Where T is the return period in question.

Thus, the values of maximum daily rainfall are calculated for several return periods.

2.5. Correlation of durations

Since the IDF curves require intensities for durations shorter than 24 hours, usually starting from 5 minutes, its ratios were obtained from rain gauge data. For this rainfall station, there is also has data from rain gauge which allows the development of the disaggregation factors shown in Figure 6.

Preprints (www.preprints.org) | NOT PEER-REVIEWED | Posted: 4 April 2018 doi:10.20944/preprints201804.0055.v1

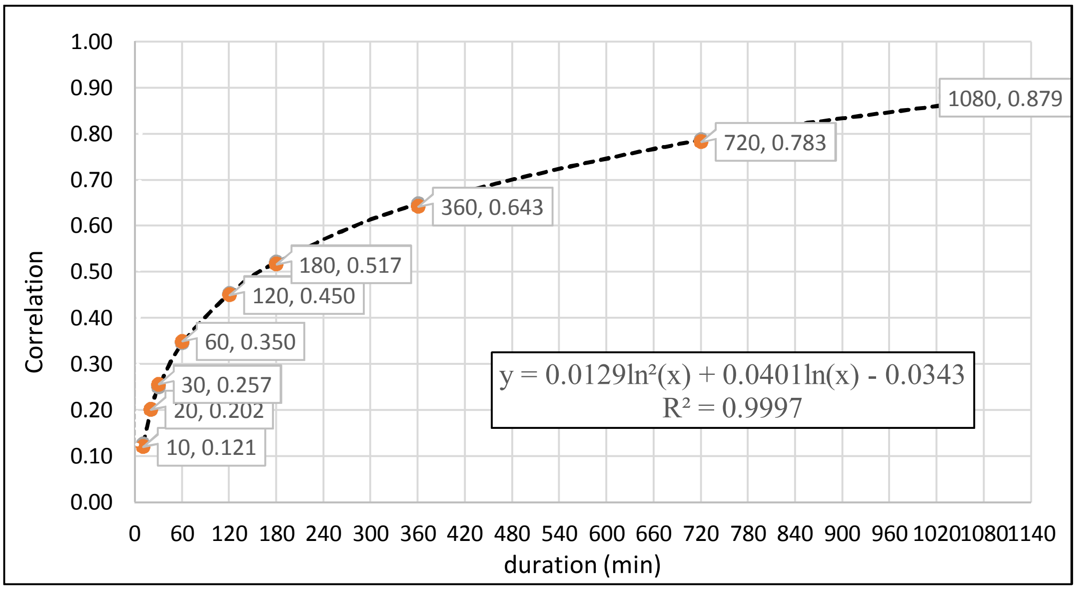

Figure 5: Correlation of durations observed in rain gauge E2-046 between 1971 and 2001 [30] minutes.

In Brazil is relatively easy to obtain daily rainfall data, but rainfall data of shorter duration are rarely available, due to the lack of recording equipment, and when they do exist, they present relatively short series with many gaps [3].

According to CETESB [6], in 1966 the Agronomic Research Institute conducted a study aiming to establish a relationship between the maximum rainfalls for "1 day" (pluviometers) and "24 hours" (pluviographs), based on annual series covering the period from 1928 until 1965, obtaining values from 1.13 to 1.15 for different return periods. These values 1 day/24 hours are different because they represent correlations between data from pluviometers (1 day) and pluviographs (24 hours). The daily precipitation corresponds to the value between the rainfall of two fixed observation hours, while 24 hours of rainfall is the highest value corresponding to rain a consecutive period of 24 hours. For this work, the average of these correlations is used, 1.036. This coefficient is used to convert 1-day precipitation into 24-hour precipitation.

3. Results and Discussion

3.1. Analysis of comparative frequency, between Model and Rain Gauge Data

The frequency distribution for the two data sets of daily precipitation, Eta RCM precipitation data and observed data, is shown in Figure 6. Is possible to notice that there are outliers above 180mm/per day in the observed data, as they did no pass on the test proposed by Rosner [44] by a significance of 5%.

In fact, the correlation for values above 120 just seems to be poor. However, the problem is that, as a supposedly random distribution, the absence or the presence of data at the histogram depends on the expected value of the accumulated distribution.

For example, when one takes 16500 random values distributed by a gamma with κ=0.631552 and θ=22.87797, although the expected number of values between 140 and 150 is 2.88, a random distribution may produce no values at this interval. Figure 6 shows two Monte Carlo [2, 21] random distributions plotted against the theoretical histogram. The "experimental" histogram might be interpreted as a "poor" representation of the gamma distribution, although it was generated to follow that gamma.

Preprints (www.preprints.org) | NOT PEER-REVIEWED | Posted: 4 April 2018 doi:10.20944/preprints201804.0055.v1

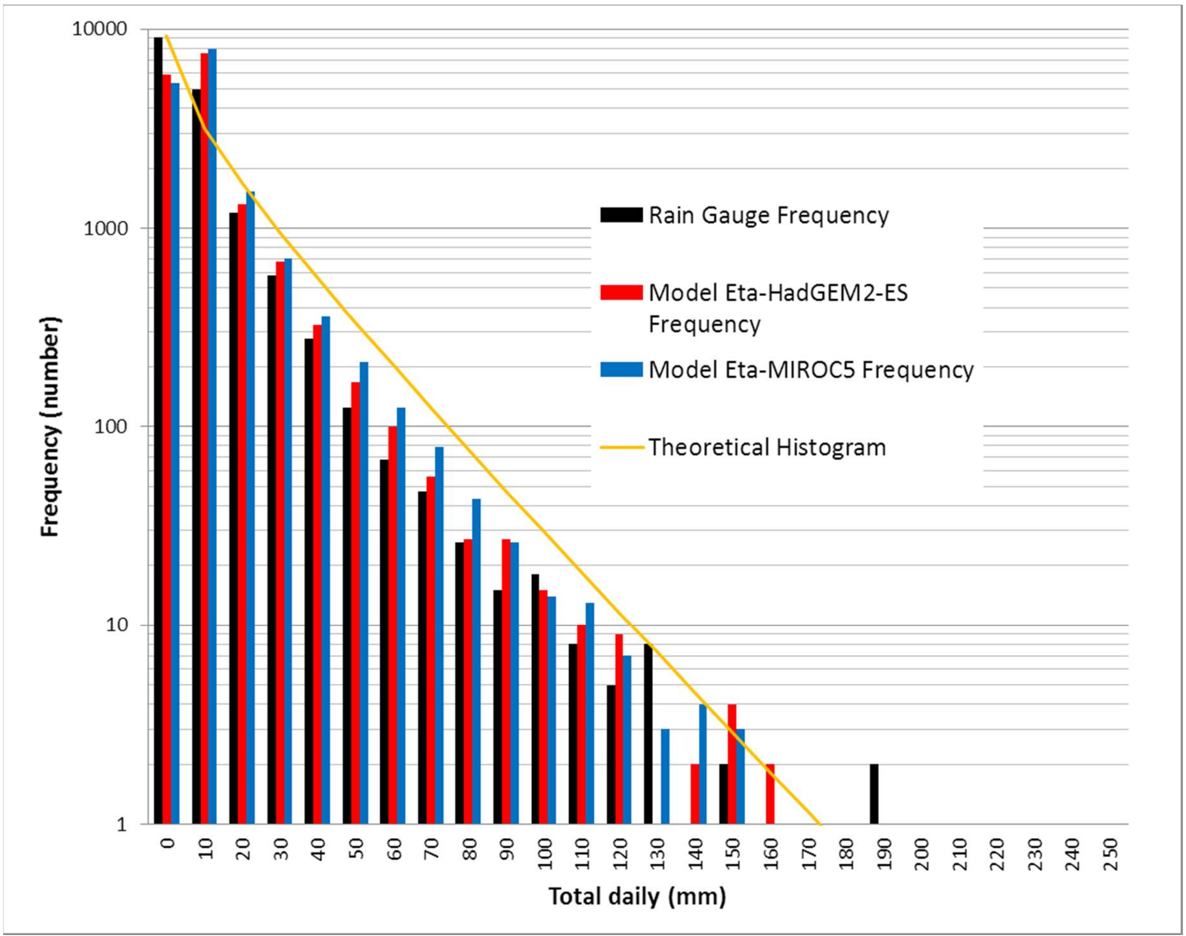

Figure 6: Analysis of total daily precipitation frequency for station E2-046 and both Eta RCM between 1961 and 2005 with the presence of the theoretical histogram.

From this analysis, it can be seen that the data have a high correlation and therefore can generate consistent annual maximum rainfall data, permitting the comparison of the curves generated by the rain gauge station and by the Eta-HadGEM2-ES and Eta-MIROC5 RCM.

3.2. IDF Curve for rain gauge station

Using the Gumbel distribution fitted to the observed data set, the parameters α and β were obtained and used to generate the daily precipitation values for return periods (T) of 2, 5, 10, 15, 20, 25, 50 and 100 years, respectively, as shown in Table 2:

Table 2: Calculation of maximum daily rainfall (mm), for several return periods using Gumbel distribution fitted to rain gauge station:E2-046: Caraguatatuba/SP.

Variable	Values obtained using the Gumbel distribution							
β	31,44							
α	86,79							
T	2	5	10	15	20	25	50	100
F (1 day;T)	0,50	0,80	0,90	0,93	0,95	0,96	0,98	0,99
P (1 day; T) mm	98,31	133,94	157,53	170,84	180,16	187,34	209,46	231,41

Disaggregating the maximum daily rainfall into durations of 24h, 12h, 8h, 6h, 2h, 1h, 30 min, 25 min, 20 min, 15 min, 10 min and 5 min, as described previously, it was obtained the precipitation amounts showed in Table 3:

Preprints (www.preprints.org) | NOT PEER-REVIEWED | Posted: 4 April 2018 doi:10.20944/preprints201804.0055.v1

Table 3: Precipitation amounts (mm) obtained for rain gauge station: E2-046: Caraguatatuba/SP.

			Retun Period							
Rainfall Duration	Rainfall Duration (min)	Relation Between Rainfall	2	5	10	15	20	25	50	100
5 min	5	0,064	6,26	8,53	10,03	10,87	11,47	11,92	13,33	14,73
10 min	10	0,126	12,43	16,93	19,92	21,60	22,78	23,69	26,48	29,26
15 min	15	0,169	16,60	22,62	26,61	28,85	30,43	31,64	35,38	39,08
20 min	20	0,202	19,82	27,00	31,76	34,44	36,32	37,77	42,23	46,65
25 min	25	0,228	22,46	30,60	35,99	39,03	41,16	42,80	47,85	52,86
30 min	30	0,251	24,71	33,66	39,59	42,94	45,28	47,08	52,64	58,16
1 hour	60	0,346	34,03	46,36	54,53	59,14	62,36	64,85	72,50	80,10
2 hours	120	0,453	44,57	60,72	71,42	77,45	81,68	84,93	94,96	104,91
6 hours	360	0,649	63,77	86,88	102,19	110,82	116,87	121,52	135,87	150,11
8 hours	480	0,705	69,30	94,42	111,06	120,44	127,01	132,07	147,66	163,13
10 hours	600	0,750	73,74	100,47	118,17	128,15	135,14	140,52	157,11	173,58
12 hours	720	0,788	77,46	105,54	124,13	134,61	141,96	147,61	165,04	182,33
24 hours	1440	1,036	101,85	138,76	163,21	177,00	186,65	194,09	217,00	239,74
1 day		1	98,31	133,94	157,53	170,84	180,16	187,34	209,46	231,41

These observed data are shown in the form of IDF curves in Figure 7.

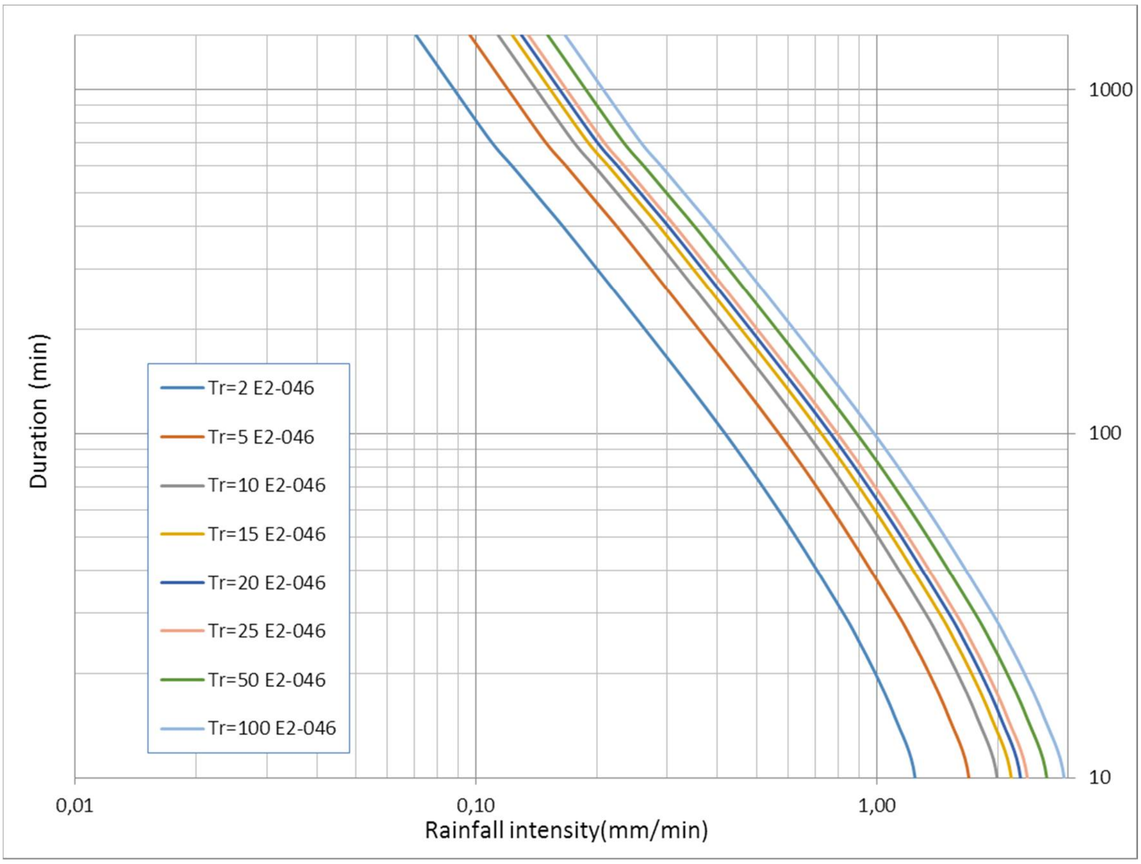

Figure 7: IDF curves in a logarithmic scale for different durations and different return periods for rain gauge E2-046: Caraguatatuba/SP.

3.3. IDF Curves from Eta RCM simulation data: Control Period 1961-2005

After processing the data, IDF curves for the Eta-HadGEM2-ES and Eta-MIROC5 were determined using the same methodology employed to the observed data.

Preprints (www.preprints.org) | NOT PEER-REVIEWED | Posted: 4 April 2018 doi:10.20944/preprints201804.0055.v1

The daily precipitation for return periods (T) of 2, 5, 10, 15, 20, 25, 50 and 100 years is shown in Table 4 and 6:

Table 4: Calculation of maximum daily rainfall (mm), for several return periods using Gumbel distribution from Eta-HadGEM2-ES data.

Variable	**Values obtained using the Gumbel distribution**							
β	24,57							
α	83,50							
T	2	5	10	15	20	25	50	100
F (1 day;T)	0,50	0,80	0,90	0,93	0,95	0,96	0,98	0,99
P (1 day; T) mm	92,50	120,35	138,79	149,19	156,47	162,08	179,36	196,52

Disaggregating the maximum daily rainfall into 24h, 12h, 8h, 6h, 2h, 1h, 30 min, 25 min, 20 min, 15min, 10 min and 5 min, it was obtained the precipitation amounts showed in Table 5 and 7.

Table 5: Precipitation amounts (mm) obtained from the Eta-HadGEM2-ES data.

			Retun Period							
Rainfall Duration	Rainfall Duration (min)	Relation Between Rainfall	2	5	10	15	20	25	50	100
5 min	5	0,064	5,89	7,66	8,83	9,50	9,96	10,32	11,42	12,51
10 min	10	0,126	11,70	15,22	17,55	18,86	19,78	20,49	22,68	24,85
15 min	15	0,169	15,62	20,33	23,44	25,20	26,43	27,38	30,29	33,19
20 min	20	0,202	18,65	24,26	27,98	30,08	31,54	32,68	36,16	39,62
25 min	25	0,228	21,13	27,49	31,70	34,08	35,74	37,03	40,97	44,89
30 min	30	0,251	23,25	30,25	34,88	37,49	39,32	40,73	45,08	49,39
1 hour	60	0,346	32,02	41,66	48,04	51,64	54,16	56,10	62,08	68,02
2 hours	120	0,453	41,94	54,56	62,92	67,63	70,94	73,48	81,31	89,09
6 hours	360	0,649	60,00	78,07	90,03	96,77	101,50	105,14	116,35	127,48
8 hours	480	0,705	65,21	84,84	97,84	105,17	110,31	114,26	126,44	138,54
10 hours	600	0,750	69,39	90,27	104,10	111,91	117,37	121,58	134,54	147,41
12 hours	720	0,788	72,89	94,83	109,35	117,55	123,29	127,71	141,33	154,84
24 hours	1440	1,036	95,83	124,68	143,78	154,56	162,11	167,92	185,82	203,59
1 day		1	92,50	120,35	138,79	149,19	156,47	162,08	179,36	196,52

Table 6: Calculation of maximum daily rainfall (mm), for several return periods using Gumbel distribution from Eta-MIROC5 data.

Variable	**Values obtained using the Gumbel distribution**							
β	18,76							
α	87,43							
T	2	5	10	15	20	25	50	100
F (1 day;T)	0,50	0,80	0,90	0,93	0,95	0,96	0,98	0,99
P (1 day; T) mm	94,31	115,58	129,66	137,60	143,16	147,45	160,64	173,74

Table 7: Precipitation amounts (mm) obtained from the Eta-MIROC5 data.

			Retun Period							
Rainfall Duration	Rainfall Duration (min)	Relation Between Rainfall	2	5	10	15	20	25	50	100
5 min	5	0,064	6,00	7,36	8,25	8,76	9,11	9,39	10,23	11,06
10 min	10	0,126	11,92	14,61	16,39	17,40	18,10	18,64	20,31	21,97
15 min	15	0,169	15,93	19,52	21,90	23,24	24,18	24,90	27,13	29,34
20 min	20	0,202	19,01	23,30	26,14	27,74	28,86	29,72	32,39	35,03
25 min	25	0,228	21,54	26,40	29,62	31,43	32,70	33,68	36,70	39,69
30 min	30	0,251	23,70	29,05	32,58	34,58	35,98	37,06	40,37	43,66
1 hour	60	0,346	32,64	40,00	44,88	47,63	49,55	51,04	55,60	60,14
2 hours	120	0,453	42,76	52,40	58,78	62,38	64,90	66,84	72,83	78,77
6 hours	360	0,649	61,18	74,97	84,10	89,26	92,86	95,64	104,20	112,70
8 hours	480	0,705	66,49	81,48	91,40	97,00	100,92	103,94	113,25	122,48
10 hours	600	0,750	70,74	86,69	97,25	103,21	107,38	110,60	120,50	130,32
12 hours	720	0,788	74,31	91,07	102,16	108,42	112,80	116,18	126,57	136,90
24 hours	1440	1,036	97,71	119,74	134,32	142,55	148,32	152,75	166,43	180,00
1 day		1	94,31	115,58	129,66	137,60	143,16	147,45	160,64	173,74

These model–derived data are shown in the form of IDF curves in associated with observed IDF in Figure 8. It shows 5, 10, 50 and 100-year IDF curves respectively for rain gauge E2-046 and the Eta-HadGEM2-ES and Eta-MIROC5 RCM model interpolated to the gauge location. The curves are distant from the IDF observed but the curve of Eta-HadGEM2-ES is closer than Eta-MIROC5. The discrepancy between the expected and observed data is of a modest magnitude.

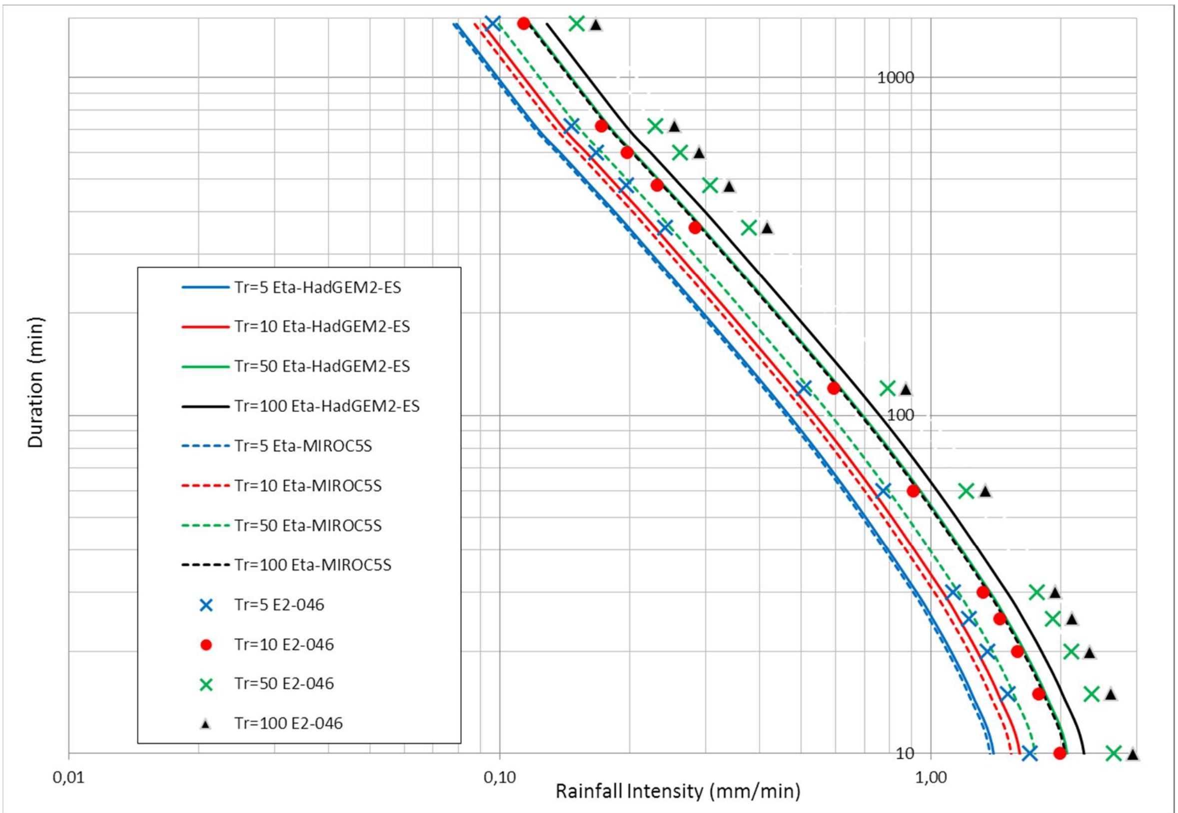

Figure 8: IDF curves for different durations and different return periods for observed data of rainfall station E2-046 and Eta-HadGEM2-ES/MIROC5 in logarithmic scale interpolated to the location of rain gauge E2-046.

Preprints (www.preprints.org) | NOT PEER-REVIEWED | Posted: 4 April 2018 doi:10.20944/preprints201804.0055.v1

Furthermore, Figures 9 and 10 show points on the 10-year and 100-year IDF curves respectively for rain gauge E2-046 and the Eta RCM model interpolated to the gauge location. One notices that the curves with a return period of 10 years are very close to each other. However, for the curves for a higher return period, namely 100 years, as shown in Figure 10, the values are slightly different for shorter duration. The Eta-MIROC5 tends to underestimate the results, while the Eta-HadGEM2-ES tends to be closer to the observed data. At last, models are usually unable to predict outliers, which may have real causes in rare events or may be due to wrong measurements.

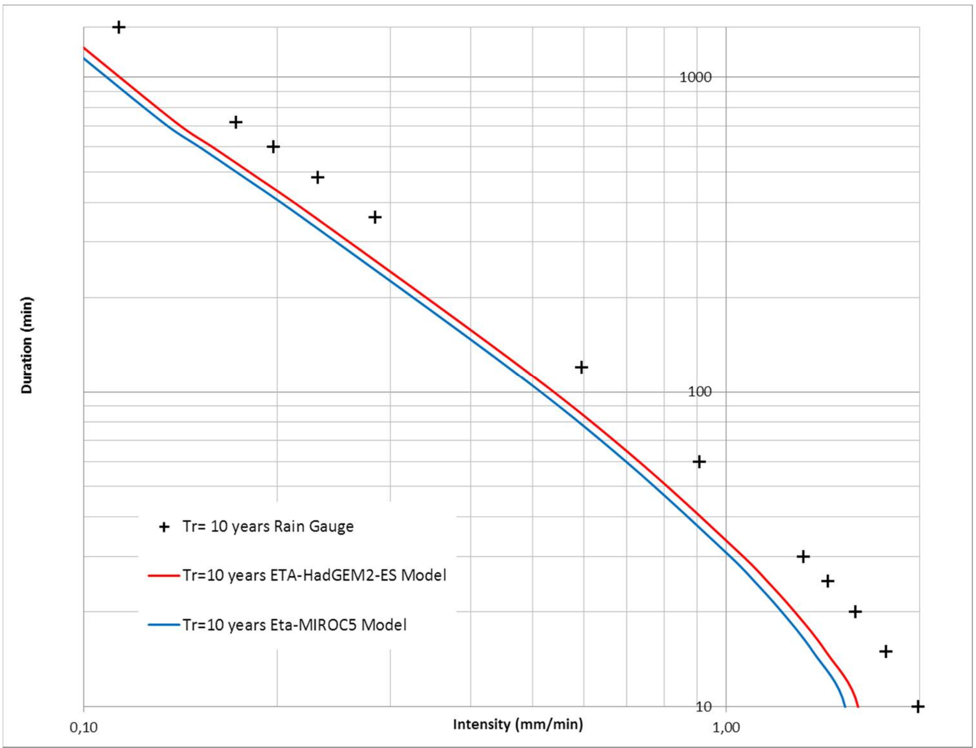

Figure 9: Values of the average rainfall intensity for rain gauge and Eta-HadGEM2-ES and Eta-MIROC5 in relation to the rain gauge E2-046 for return period of 10 years.

Preprints (www.preprints.org) | NOT PEER-REVIEWED | Posted: 4 April 2018 doi:10.20944/preprints201804.0055.v1

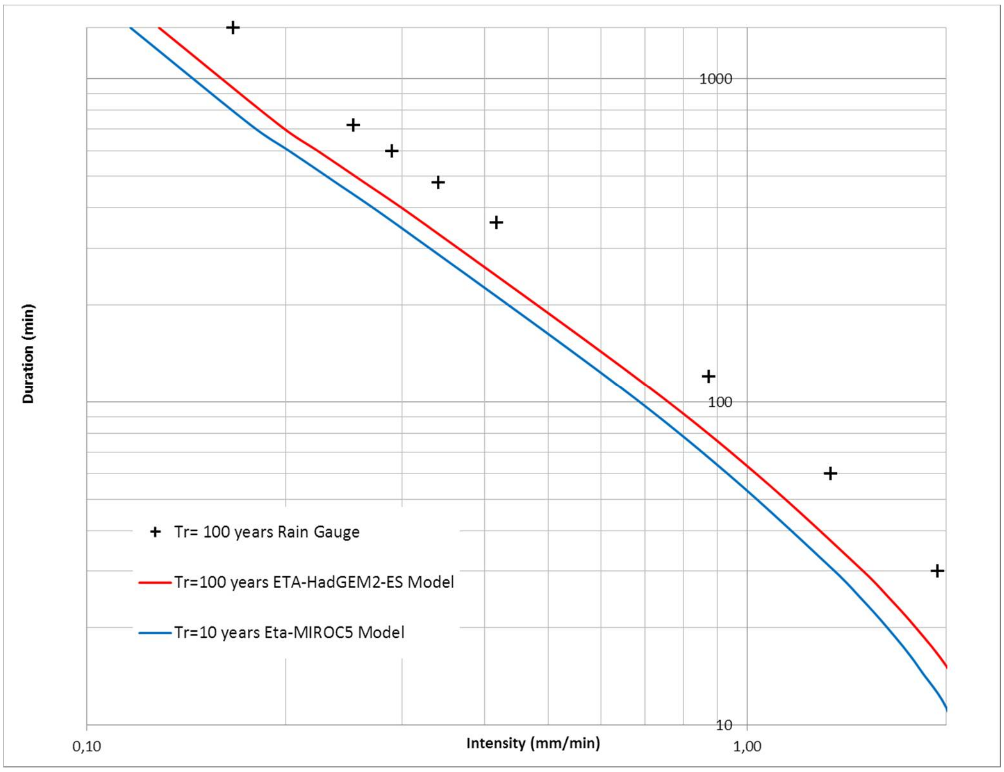

Figure 10: As in Fig 7, but for return period of 100 years.

4. Conclusions

The design of a drainage structure must be closely related to local hydrological data. This study compared rain gauge E2-046 data and Eta RCM precipitation data for the purpose of generating IDF curves to assist in design of drainage structures. This work is relevant because there are no reliable IDF curves for Caraguatatuba, so that the designers have been using IDF curves from Ubatuba, a nearby town.

From the frequency analysis, comparing the rain gauge (E2-046) and Eta RCM (Eta-HadGEM2-ES and Eta MIROC5) for the same point, one can see that the IDF curves almost overlap as shown Figure 8, 9 and 10. Furthermore, correcting bias was fundamental because the method reduces the systematic errors produced by the Eta RCM.

The IDF curves presented are practically identical for a return period of 10 years, but when the return period increases to 100 years, the intensities of short duration tend to be higher for the IDF from model data than for the IDF from observed data, based on 31 years of data (control period).

The results present a very good correlation between the two IDF curves for the control period (1961-2005), indicating the possibility of using the Eta RCM precipitation forecasts from 2007 - 2099 to establish a future IDF and thereby, allowing the consideration of climate changes in urban drainage design.

Despite complex, this methodology has the objective of validate regional models from observed data giving opportunity for the generation of future curves. It should be noticed that the displacement among these curves do not change the drainage projects both large and small projects.**Acknowledgments:** The authors would like to thank the Rede Litoral Project, "Mudanças climáticas globais e impactos na zona costeira: modelos, indicadores, obras civis e fatores de mitigação/adaptação - REDELITORAL NORTE SP", CAPES 417/2010 (http://www.redelitoral.ita.br/); the National Institute for Space Research (INPE, São Paulo, Brazil) for providing the Eta Regional Climate Model data (http://www.inpe.br/), and special persons Engineers Nelson Luiz Goi Magni and Maria Laura Centini Gói from Departamento de Águas e Energia Elétrica do Estado de São Paulo (http://www.daee.sp.gov.br/).

Author Contributions: Daniela Martins led the design of the proposed methodology, performed the numerical calculations, and participated in the analysis and discussion of results and paper writing. Nadiane Smaha Kruk contributed to the general idea of the research, participated in the analysis and discussion of the results, and

Preprints (www.preprints.org) | NOT PEER-REVIEWED | Posted: 4 April 2018 doi:10.20944/preprints201804.0055.v1

contributed to the writing. Paulo Ivo Braga de Queiroz and Gabriele Vanessa Tschöke contributed to the methodology of bias correction. Wilson Cabral de Souza Júnior was the general coordinator of the Rede Litoral project and created a network of research on global changes and impacts on coastal regions.

Conflicts of Interest: The authors declare no conflict of interest.

References

1. Agilan, V. and Umamahesh, N. M. Is the covariate based non-stationary rainfall IDF curve capable of encompassing future rainfall changes? *Journal of Hydrology* (**2016**) 541, 1441–1455.
2. Ang, A. H-S and Tang, W. H. *Probability Concepts in Engineering Planning and Design – Volume II Decicsion, Risk, and Reliability* (**1990).** Copyright Ang & Tang.
3. Back, Á. J., Uggioni, E., Vieira, H. J.: Modeling precipitation of short duration by means of the Modified Bartlett-Lewis Rectangular Pulse Model. *Revista Brasileira de Meteorologia* (**2011)** v.26, n.3, 461-472.
4. Bourdages, L., Huard, D.: Climate Change Scenario over Ontario Based on the Canadian Regional Climate Model (CRCM4.2). *Report of Consortium on Regional Climatology and Adaptation to Climate Chang*e. (**2010**) <www.Quranos.ca>.
5. CETESB: **1980**. *Drenagem Urbana: Manual de Projeto*. São Paulo, DAEE/CETESB. 468p.
6. Chou, S.C.; Lyra, A.; Mourão, C.; Dereczynski, C.; Pilotto, I.; Gomes, J.; Bustamante, J.; Tavares, P.; Silva, A.; Rodrigues, D.; Campos, D.; Chagas, D.; Sueiro, G.; Siqueira, G. and Nobre, P (**2014a**). Assessment of Climate Change over South America under RCP 4.5 and 8.5 Downscaling Scenarios. *American Journal of Climate Change*, 2014, 3, 512-525.
7. Chou, S.C.; Lyra, A.; Mourão, C.; Dereczynski, C.; Pilotto, I.; Gomes, J.; Bustamante, J.; Tavares, P.; Silva, A.; Rodrigues, D.; Campos, D.; Chagas, D.; Sueiro, G.; Siqueira, G. e Nobre, P (**2014b**). Evaluation of the Eta simulations nested in three global climate models. *American Journal of Climate Change*, 2014.
8. Chow, V. T.; Maidment, D. R. and Mays, L. W. *Applied Hydrology*. New York: McGraw-Hill, **1988**.
9. Collins, W.J., et al.: Development and Evaluation of an Earth-System Model—HadGEM2. *Geoscientific Model Development*, (**2011**) 4, 1051-1075, http://dx.doi.org/10.5194/gmd-4-1051-2011
10. Ek, M. B.; Mitchell, K. E.; Lin, Y.; Rogers, E.; Grunmann, P.; Koren, V.; Gayno, G. and Tarpley, J. D. Implementation of Noah land surface model advances in the National Centers for Environmental Prediction operational mesoscale Eta model, *J. Geophys. Res.*, 108, 8851, (**2003**)
11. Fels, S. B. and Schwarzkopf, M. D. The Simplified Exchange Approximation: A New Method for Radiative Transfer Calculations. J. Atmos. Sci., 32, 1475–1488, (**1975**).
12. Gadd, A. J. A split-explicit integration scheme for numerical weather prediction. *Quart. J. Roy. Met. Soc.*, 104, 569-582 (**1978**).
13. Gumbel, E. J. *Statistics of Extremes*. New York: Columbia University Press, (**1958)**.
14. Haan, C.T.: *Statistical Methods in Hydrology*. Ames, IO: University Press , **1977**. 378 p., il., 23 cm. ISBN 0-8138-1510-X.
15. IPCC: *Climate Change 2013: The Physical Science Basis. Contribution of Working Group I to the Fifth Assessment Report of the Intergovernmental Panel on Climate Change*. (**2013**) Cambridge University Press, Cambridge, United Kingdom and New York.
16. IPCC: *Climate Change 2014: Synthesis Report. Contribution of Working Groups I, II and III to the Fifth Assessment Report of the Intergovernmental Panel on Climate Change.* (**2014**) [Core Writing Team, R.K. Pachauri and L.A. Meyer (eds.)]. IPCC, Geneva, Switzerland, 151 pp.
17. Janjíc, Z.I. Forward-backward scheme modified to prevent two-grid-internal noise and its application in sigma coordinate models. *Contrib. Atmos. Phys.*, 52, 69-84, (**1979**).
18. Janjíc, Z.I. The step-mountain Eta coordinate Model: Further developments of the convection, viscous sublayer, and turbulence closure schemes. *J. Atmos. Sci.*, 122, 927-945, (**1994**).
19. Kao, S.C.; Ganguly, A.R. Intensity, duration, and frequency of precipitation extremes under 21st-century warming scenarios, *J. Geophys. Res*. (**2011**), 116, D16119, doi:10.1029/2010JD015529.
20. Karam, H.A., Pereira Filho, A.J., Masson, V., Noilhan, J. and Marques Filho, E. P. Formulation of a tropical town energy budget (t-TEB) scheme, *Theor Appl Climatol*, 101: 109, (**2010**).
21. Kottegoda, N. T. and Rosso, R. *Statistics, Probability, and Reliability for Civil and Environmental Engineers*. New York: McGraw-Hill, **1997**.
22. Kuo C.C., Gan P., Hanraran, J. L. Precipitation frequency analysis based on regional climate simulations in Central Alberta. *Journal of Hydrology* (**2014**) 510, 436-446.

Preprints (www.preprints.org) | NOT PEER-REVIEWED | Posted: 4 April 2018 doi:10.20944/preprints201804.0055.v1

23. Lacis, A. A. and Hansen, J. A Parameterization for the Absorption of Solar Radiation in the Earth's Atmosphere. *J. Atmos. Sci*., 31, 118–133, (**1974**).
24. Liew, S.C., Liong, S-Y. and V. Raghavan, S. A novel approach, using regional climate model, to derive present and future IDF curves for data scarce sites. 18th *Congress of International Association of Hydraulics Engineering and Research – Asia Pacific Division* (**2012**) (Best Paper Award).
25. Madsen, H.; Arnbjerg-Nielsen, K.; Mikkelsen, P. S. Update of regional intensity–duration–frequency curves in Denmark: Tendency towards increased storm intensities. *Atmospheric Research* (**2009**) 92, 343–349.
26. Magni, N.l.G. Estudo Pontual de Chuvas Intensas: Proposição e Análise de Uma Metodologia de Estudo das Relações Intensidade-Duração-Frequência Definidas para Um Ponto. *Dissertação apresentada à Escola de Politécnica da Universidade de São Paulo, para obtenção do título de Mestre em Engenharia. São Paulo* (**1984)** 156p.
27. Mailhot, A.; Duchesne, S.; Caya, D.; Talbot, G. Assessment of future change in intensity–duration–frequency (IDF) curves for Southern Quebec using the Canadian Regional Climate Model (CRCM). *Journal of Hydrology* (**2007**) 347, 197-210.
28. Martin, G.M., et al.: **2011**. The HadGEM2 Family of Met Office Unified Model Climate Configurations. *Geoscientific Model Development*, 4, 723-757, http://dx.doi.org/10.5194/gmd-4-723-2011
29. Martins, D.; Kruk, N. S.; Magni, N. L. G. and Queiroz, P. I. B. Comparison of two methods for the determination of the intense rainfall equation for Caraguatatuba (SP). *DAE Journal* 207 (5): 34-49. (**2017**).
30. Martins, D.; Queiroz, P. I. B, Gandini, M. L. T. and Kruk, N. S. Disaggregation of daily rainfall data to Caraguatatuba city, north coast of São Paulo. *DAE Journal.* "to appear in"
31. Masson, V; Marchadier, C.; Adolphe, L.; Aguejdad, R.; Avner, P.; Bonhomme, M.; Bretagne, G.; Briottet, X.; Bueno, B.; Munck, C.; Doukari, O.; Hallegatte, S.; Hidalgo, J.; Houet, T.; Le Bras, J.; Lemonsu, A.; Long, N.; Moine, M.; Morel, T.; Nolorgues, L.; Pigeon, G. Adapting cities to climate change: A systemic modelling approach. *Urban Climate* (**2014**) v.10, p. 407-429.
32. Mirhosseini, G.; Srivastava, P. and Stefanova, L. The impact of climate change on rainfall Intensity–Duration–Frequency (IDF) curves in Alabama. *Reg Environ Change* (**2012**). DOI 10.1007/s10113-012-0375-5
33. Mirzaei, P. A. Recent challenges in modeling of urban heat island, *Sustainable Cities and Society*, Volume 19, Pages 200-206, (**2015**).
34. Moss, R.H., Edmonds, J.A., Hibbard, K.A., Manning, M.R., Rose, S.K., Vuuren, D.P.V, Carter, T.R., Emori, S., Kainuma, M., Kram, T., Meehl, G.A., Mitchel, J.F.B., Nakicenovic, N., Riahi, K., Smith, S.J., Stouffer, R.J., Thomson, A.M., Weyant, J.P. and Wilbanks, T.J. 2010. The next generation of scenarios for climate change research and assessment. *Nature Magazine*, Vol 463, 747-756 (**2010)**. doi:10.1038/nature08823
35. Naghettini, M.; Pinto, E. J. A. *Hidrologia estatística*. (**2007**) Belo Horizonte: CPRM. 552 p.
36. National Research Council. (United States) *Informing decisions in a changing climate: panel on strategies and methods for climate-related decision support*. Washington, D.C.: The National Academies Press (**2009)**. 201p.
37. Occhipinti, A. G., Santos, P. M. Relação entre as precipitações máximas de "um dia" e de "24 horas" na cidade de São Paulo. *III Simpósio de Redes Hidrológicas*, 1º, Belo Horizonte, 13p., (**1966**).
38. PBMC: *Contribuição do Grupo de Trabalho 1 ao Primeiro Relatório de Avaliação Nacional do Painel Brasileiro de Mudanças Climáticas. Sumário Executivo GT1*. (**2013**) Brazilian Panel for Climate Changes (Painel Brasileiro de Mudanças Climáticas – PBMC), Rio de Janeiro, Brasil, 24p. ISBN: 978-85-285-0208-4
39. Prodanovic, P., Simonovic, S.P. Development of Rainfall Intensity Duration Frequency Curves for the City of London Under the Changing Climate, *Water Resources Research Report-Report nº 058*. (**2007**). The University of Western Ontario, Ontario, Canada.
40. Projeta. Available online: https://projeta.cptec.inpe.br (accessed on 14 January 2018).
41. Rana, A., Foster, K., Bosshard, T., Olssonb, J., Bengtssona, L. 2014. Impact of climate change on rainfall over Mumbai using Distribution-based Scaling of Global Climate Model projections. *Journal of Hydrology: Regional Studies*. 1 (**2014**) 107–128.
42. Righetto, A. M. *Hidrologia e Recursos Hídricos*. (**1998**) São Paulo: EESC-UPS. 819 p.
43. Rodríguez, R., Navarro, X., Casas, C. C., Ribalaygua, J., Russo, B. Pougetd, L. and Rodriguez, A. R. Influence of climate change on IDF curves for the metropolitan area of Barcelona (Spain). *Int. J. Climatol*. (**2013**). Published online in Wiley Online Library (wileyonlinelibrary.com) DOI: 10.1002/joc.3712
44. Rosner, B. Percentage Points for a Generalized ESD Many-Outlier Procedure, *Technometrics*, 25:2, 165-172, (**1983**).

Preprints (www.preprints.org) | NOT PEER-REVIEWED | Posted: 4 April 2018 doi:10.20944/preprints201804.0055.v1

45. Shrestha, A; Babel, M. S.; Weesakul, S. and Vojinovic, Z.: 2017. Developing Intensity–Duration–Frequency (IDF) Curves under Climate Change Uncertainty: The Case of Bangkok, Thailand. *Water*. (**2017**); 9(2):145. doi:10.3390/w9020145.
46. Solaiman, T. A. and Simonovic, S. P. Development of Probability Based Intensity – Duration -Frequency Curves under Climate Change. *Water Resources Research Report,* (**2011**) Book 34. <http://ir.lib.uwo.ca/wrrr/34>
47. Sordo-Ward, A; Bejarano, M. D.; Iglesias, A.; Asenjo, V. and Garrote, L.: 2017. Analysis of Current and Future SPEI Droughts in the La Plata Basin Based on Results from the Regional Eta Climate Model. *Water*. (**2017**); 9, 857; doi:10.3390/w9110857.
48. Srivastav, R. K., Schardong, A., Simonovic, S.P. Equidistance Quantile Matching Method for Updating IDF Curves under Climate Change. *Water Resour Manage*, (**2014).** DOI 10.1007/s11269-014-0626-y
49. Tschöke, G.V., Kruk, N.S., de Queiroz, P.I.B.; Sousa Júnior,W.C. Comparison of two bias correction methods for precipitation simulated with a regional climate model. *Theoretical and Applied Climatology* (**2015**). doi:10.1007/s00704-015-1671-z
50. Vasiljevic, B.; McBean, E. and Gharabaghi, B. Trends in rainfall intensity for stormwater designs in Ontario. *Journal of Water and Climate Change* (**2011**) Res. 03 (1), 1–10.
51. Watanabe, M., et al. Improved Climate Simulation by MIROC5: Mean States, Variability, and Climate Sensitivity. *Journal of Climate*, (**2010**) 23, 6312-6335. http://dx.doi.org/10.1175/2010JCLI3679.1
52. Willems, P. "Revision of urban drainage design rules after assessment of climate change impacts on precipitation extremes at Uccle, Belgium". *Journal of Hydrology* (**2013)** 496, 166-177.
53. Zhao, Q, Black, TL and Baldwin M. E. Implementation of the cloud prediction scheme in the Eta Model at NCEP. *Weather and Forecasting*, 12, 697-712, (**1997**).